



REGULAR ARTICLE

Size-Dependent Physical Properties of Metallic Films: Analysis of Thermal and Mechanical Characteristics in the Nanoscale Regime

S.R. Thorat<sup>1,\*</sup> , V.M. Tidake<sup>2</sup>, P.M. Patore<sup>1</sup>, P.B. Khatkale<sup>3</sup>, A.A. Khatri<sup>4</sup>, P.M. Yawalkar<sup>5</sup>, S.S. Ingle<sup>1</sup>

<sup>1</sup> Department of Mechanical Engineering, Sanjivani College Engineering, Kopergaon, SPPU, Pune, India

<sup>2</sup> Department of MBA, Sanjivani College of Engineering, Kopergaon, SPPU, Pune, India

<sup>3</sup> Sanjivani University, Kopergaon, MH, India

<sup>4</sup> Department of Computer Engineering, Jaihind College of Engineering, Kuran, SPPU, Pune, MH, India

<sup>5</sup> Department of Computer Engineering, MET's Institute of Engineering, Nashi, India

(Received 16 April 2024; revised manuscript received 20 June 2024; published online 28 June 2024)

Metallic films, which are thin layers of metal deposited on surfaces, have a wide range of uses in many sectors. Metallic films are usually produced by sputtering or chemical vapor deposition and serve an important role in electronics, optics and coatings. Their fundamental conductivity, reflective qualities and adaptability makes important for the development of innovative materials and systems. Investigations are conducted on the rigidity, optical reflecting power, temperature conductivity and power mobility of metallic films. These attributes are affected by layer thickness, composition and deposition processes. Understanding the complexities of these physical features is critical for modifying metallic films to particular applications, which drives technological and material science innovation. In this research, the physical characteristics of metallic films, which are thinner than 20 – 200 nm were evaluated. The suggested methods for determining the Cu, and Al films temperature-dependent coefficients of resistance, thermal conductivity properties, particular heat and thermal diffusivity. The rapid amount of heating that is observed in a brief period allows the thermal characteristics of the metallic layer to be primarily evaluated without impacting the substrate.

**Keywords:** Metallic films, Thermal characteristics, Mechanical characteristics, Nanoscale materials.

DOI: [10.21272/jnep.16\(3\).03014](https://doi.org/10.21272/jnep.16(3).03014)

PACS numbers: 73.22. – f, 81.07.Bc

1. INTRODUCTION

The class of materials restricted to the nano-scale that are called low-dimensional nanostructures these materials have fewer dimensions than others. It is anticipated that bulk materials and low-dimensional nanostructures would exhibit the properties due to the distinct quantum enforcing surface and subsurface scatterings for electron, photon, and phonon generated by the tiny scale operation. Unexpectedly, in recent years, researchers and engineers from a variety of disciplines have focused on investigating peculiar physical characteristics and transportation processes in low-dimensional nanotechnology, which can encourage innovative uses in a range of domains [1]. An understanding of heat transmission at the nanoscale is necessary for vital applications including thermal electricity for energy collection, nanoparticle-mediated thermal treatment, nano-enhanced solar panels and thermal control in integrated circuits. Mean free path (MFP) phonons have an apparent thermal barrier that is far greater than the diffusive forecasting, allowing them to travel ballistically away from their thermal origin without

dispersing [2]. To determine the volumetric growth factors from the Grüneisen percentages, advances in the study of thin film heat transmission dependency on warmth and density at elevated temperatures are needed. Thin metal sheets are used in integrated laminate buildings, this enables a coordinated process of their contraction in response to temperature variations. [3].

Interface fault states have a major impact on some kind of electrical property structure. This is because Nano-Carbon (NC) was inserted into the oxide matrix exhibit a substantial number of contact faults and a significant interface-area-to-volume ratio. In these cases, the purpose of the interface is associated critical. The substrate and NCs/oxide-matrix interfaces these interaction traps are typically found. Interface traps influence the electronic dynamics in the framework because they are in electronic contact with the supporting substrate, in contrast to the other traps found in the metal oxide matrix [4]. The alloys in question exhibit a variety of multifunctional characteristics, including thermo-electric activity, magneto-caloric conduct, shape-retention effect and half-metallic ferromagnetism (HMF).

\* Correspondence e-mail: [thoratsandipmech@sanjivani.org.in](mailto:thoratsandipmech@sanjivani.org.in)



These substances are shown by band-structure simulations to be HMF. Few years ago, Heusler substances were predicted to be half-metallic, have a high Curie-Weiss temperature ( $T_c$ ) and resemble distinct electronic components structurally. These characteristics make them the most probable class of elements for use in magneto-electronics and spin electronics [5-6]. Modeling the behavior of micro-/nano-electromechanical systems (M/NEMS) has become relevant due to its increasing uses in a variety of technical fields, including structure, legal, electricity, healthcare, and aerospace. Furthermore, precise knowledge of the physiological properties of the aforementioned structures which can be characterized in terms of cables, containers, beams, plates, and shells is necessary for modeling them [7].

## 2. RELATED WORK

The study [8] employed to use brief frequency illuminating pulses lasting femtoseconds to reveal a realm of nanoscale heat transfer that was not earlier known to exist. This domain arises when the distance between heating producers and their width are comparable to the mean free paths of the primary heat-carrying waves in the materials. The study [9] investigated that the characteristics of  $L_{12}$ -structured nano precipitates and their processes of recoveries and recrystallizing were significantly influenced by the processing regime. Enhanced regenerative tension, higher resilience and greater adaptability were achieved in pre-annealed films in two-step protocol with a prolonged ambient temperature stage, owing to the high-density distribution of nano precipitates. The relative contribution of each reinforcing mechanism was evaluated. The study [10] explained the effects of curing protocols on the moisture content, microscopic structure, and mechanical properties of Ultra-High-Performance Concrete (UHPC). The results show that increasing the degree of curing increases the material's physical properties nevertheless, unlike regular concrete, the ratio of tensile to stiffness shows an unusual tendency to increase with rising temperatures and tension strength. Additionally, heat treatment enhances the nano-mechanical properties.

The study [11] examined the low-dimensional materials' nano-mechanical characteristics and deformation processes. With a focus on empirical studies, provide an overview of the latest developments in the nano-mechanical investigations of few model 1D/2D crystalline nanostructures. By using a technique known as strain technology, the nano-mechanical process can be used to modify the functional characteristics and performance of the materials. This can lead to new research directions in developing and manufacturing devices with more drastic modifications in low-dimensional crystalline substances for utilization in interactions, processing information, biomedicine and energy. The study [12] suggested the rapid development of graphene sheets in a matter of seconds by the use of a liquid carbon source

to quench a heated steel foil. Four types of nano-crystalline material graphene films with typical particle sizes of around 3.6, 5.8, 8.0, and 10.3 nm are produced utilizing thin sheet of platinum and ethanol as substrates. It is discovered that the nano-scale size, the impact of the grain line gets more apparent. The study [13] explained the sheet with grains sized 3.6 nm shows superior Young's modulus (576 GPa) and strength (101 GPa) in comparison to pure graphene. However, its capacitance decreases by more than 100 times, indicating conductive activity with a bandgap of around 50 meV. Potential applications for rapid manufacturing of conventional graphene compounds and other 2D nano-crystalline substances include liquid-phase precursors quenching.

## 3. METHODOLOGY

### 3.1 Thermal-Electric Characteristics

The temperature coefficient of resistance ( $\alpha_s$ ) and variations in temperatures  $\Delta P$  are observed with changes in electrical resistance  $\Delta S$ , can be calculated using the following relation in Eq. (1):

$$\alpha_s = \frac{\Delta S}{S_0 \Delta P} \quad (1)$$

To achieve the modifications in resistance to electricity, a metallic film that has been formed on the surface of the glass to a confident nano thickness gets heated via the Joule effect between two metallic copper conductors. The  $K$ -type nano thermocouple is utilized to measure the internal temperature under conditions of a constant state.

### 3.2 Thermal Characteristics

Using alternating current micropulses methods, particular heat  $D_{qg}$ , heat dissipation  $E_g$ , and heat transfer coefficient  $l_r$  are determined. In this instance, a signal of electricity with heating is performed to the metallic film/substrate system with a defined depth for an interval of several nanoseconds (10 to 400  $\mu$ s). In this brief period, the heat transfers with time ( $\Delta P/\Delta s$ ) allows heating information for the film to be recorded without affecting the substrate temperature. Under these circumstances, the connection yields the  $D_{qg}$  value in Eq. (2):

$$D_{qg} = \frac{Q}{n \frac{\Delta P}{\Delta s}} \quad (2)$$

Where  $m$  is the material weight and  $Q = VI$  is the power given to the film. Conversely, the identical ( $\Delta P/\Delta s$ ) plot that was acquired for the  $D_{qg}$  measurement can be used the thermal diffusion coefficient  $E_g$  derived in Eq. (3) To get the initial phases of the film heated, which solve the limited heat solution in the transient system, involving the thermal diffusion coefficient  $E_g$ .

$$\frac{1}{E_g} \frac{\partial P}{\partial s} = \frac{\partial^2 P}{\partial y^2} \quad (3)$$

Simplifying the nonlinear equation, consider the film

with a length dimension  $F$  with period throughout the operation of the electrical pulse ( $E_p$ ) provided by Eq. (4).

$$P(F, s) = P_0 \exp(\lambda^2 E_g s) \quad (4)$$

The variable of segregation, denoted as  $\lambda^2$ , is defined in the Eq. (5)

$$\lambda^2 = \frac{\Delta P}{E_g P_0 \sqrt{\frac{E_p F e_g}{E_g}}} \quad (5)$$

The temperature gradient of the film of dimension length  $F$  throughout the transient phase is provided by Eq. (4). It includes the thermal diffusivity  $E_g$  of the film significance, but considering this equation causes temperatures to rise endlessly as time rises, it must be utilized carefully. Given the assumption that equation (4) applies in the transient regime, the thermal distribution can be written as Eq. (6)

$$\Delta P_{adf}(s) = P(F, s) - P_0 \quad (6)$$

The temperature variations of the metallic film, represented by  $\Delta P_{adf} = P - P_0$  in Eq. (6), help to determine the optimal  $E_g$  value based on the observed  $\Delta T/\Delta t$  values that are obtained by applying micropulses to different films.

$$H_c = E_g D_{qg} \rho \quad (7)$$

After obtaining the  $D_{qg}$  and  $E_g$  values, the heat conductivity  $H_c$  value of the films can be approximated using Eq. (7), in which  $\rho$  represents a metallic film's density.

### 3.3 Mechanical Characteristics

Based on extensions acquired from a substrate system, the modulus of elasticity  $K$  of the fragile films is determined. The variation in a polymeric material's stress-strain ( $\sigma - \epsilon$ ) slope the material and the analogous contour for a film or polymerized substrates provide the film's  $K$  value using the following formula in the Eq. (8).

$$\sigma(\epsilon) = \frac{1}{e_g w_g} [R_{tot}(\epsilon) - R_{sub}(\epsilon)] \quad (8)$$

Where  $F$  is the force exerted on the substrate combination ( $R_{tot}(\epsilon)$ ) and substrate ( $R_{sub}(\epsilon)$ ), and  $e_g$  and  $w_g$  are the film's breadth and thickness. The unitary plot's inclination by comparing the calculated stress value with extension ( $\epsilon = \frac{\Delta Y}{Y_0}$ ), it can determine the film's elasticity modulus.

### 3.4 Deformity Techniques on Size

Flexible stretching in metals with ultrafine grain (UFG,  $1 \mu\text{m} > d > 100 \text{ nm}$ ) is caused by the mobility and propagation of displacements that come from the manufacturers of large-scale disruptions located in the core of the grain. It has been shown that the production of fractures from internal causes stacking against

granulation boundaries (GBs) with particle widths  $d > 300 \text{ nm}$  were observed in a previous in-situ study on UFG Al throughout the loading and removing phases. Cyclic loop sources cause pile-ups, which cause displacements to be incorporated into GBs under compression.

The granules were large enough and had reasons for displacement, therefore there is no evidence of intergranular flexibility. Considering there isn't enough space for aggregate displacement generators to operate and GBs take up an extensive relation, the reduction of grain size into the domain is anticipated to cause elastic deformation via an inter-granular strategy rather than an intra-granular one. Following this, UFG aluminum slender films having an average grain dimension of 250 nm were subjected to in-situ TEM tensile studies. GB grooves, among other flaws, regulate the intergranular flexibility, which includes the deposition and rather than the kind of GBs, the mobility of displacements inside them. This process occurs in all varieties of GBs, regardless of misorientation. Furthermore, a significant portion (50–100 %) of the strain caused by plastic was retrieved after discharging in NC Al with grain diameters of 65 nm, due to the micro-plasticity and Bauschinger effect. Additionally, they discovered that distortions can be released from one GB and collected by the GB from it. According to atomic experiments, displacements that initiate at GBs are responsible for flexibility in the normalcy regime. These displacements go through the grains and eventually emerge on the opposite side of the GB.

### 3.5 Experimental Setup

A heated free-evaporation approach was used to produce the thin layers of metal ( $5.7 \times 3.5 \text{ mm}^2$ ) of Al and Cu on a substrate made of glasses or Kapton. 99.9 % purity was found in the substance sources. Utilizing a quartz crystalline detector and a Maxtek 400 administrator, the width of the thin sheet was determined on-site. The K-type micro thermocouple (KK-36363) was employed as measurement device temperatures, and an HP-6643 power supply and an HP-3456A voltmeter were utilized for measuring the  $\alpha_r$  value. Two tiny electrodes of copper, that were adhered to both extremes using silver favorable paint used to apply a current pulse of power  $U_o$  and a few nanoseconds of length to the films to elevate the ambient temperature via the Joule effect and achieve other thermal attributes. A few thermal characteristics ( $E_g, H_c$  and  $D_{qg}$ ) were found using the gradient of the heating rate. The micro-pulses were applied using an electrical system that was previously reported. Using a universal tester intended for thin metal sheets, the modulus of elasticity  $K$  was ascertained.

## 4. RESULT

### 4.1 The Coefficient of Resistance ( $\alpha_r$ ) at Temperatures

The determination of the  $\alpha_r$  coefficients for ultra thin

metallurgical films was verified using two methods: the Tellier and Tosser (T-T) model and the experimental methodology. As an indicator of the film depth and average flow proportion  $\frac{e_g}{\lambda}$ , as determined by the T-T model, the  $\frac{\alpha_r}{\alpha_{bulk}}$  ratio. Fig.1 shows the relation of thickness and mean free path.

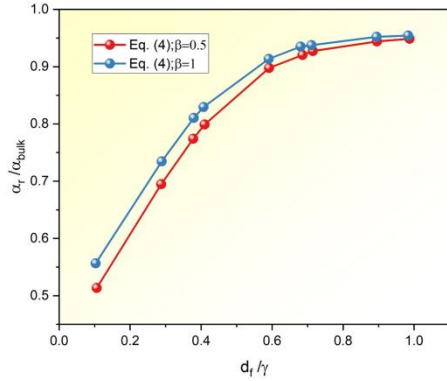


Fig. 1 – Relation of thickness of film and mean free path

It has been noted that the  $\alpha_r$  value decreases the film width ratio and the grain dimension ( $\varphi$ ), which is represented by the grain edge reflection factor ( $\beta(\varphi)$ ). This graphic enables quantitative interpolation of the  $\alpha_r$  parameter for the various film thicknesses. The equation (1) varying electrical currents delivered on each metal film to validate the  $\alpha_r$  values for various metal films frequencies that were recorded and used to determine the equivalent resistance to electricity. Fig. 2 shows the Al and Cu film  $\alpha_r$  values obtained by experimentation.

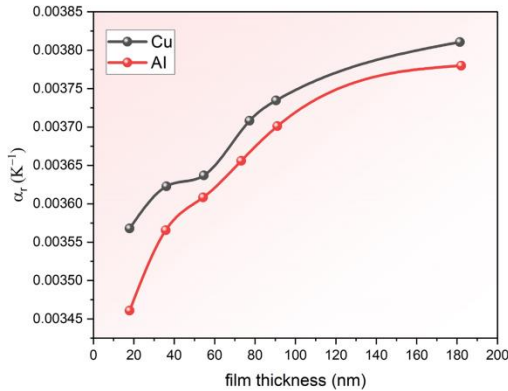


Fig. 2 – Measurement of  $\alpha_r$

Each film's rising temperature was recorded using a tiny K-type thermocouple. The observed  $\alpha_r$  values for layers of Al and Cu with widths ranging from 20 to 200 nm are displayed in Fig. 2. The theoretical and empirical  $\alpha_r$  values differed by 4%, indicating a strong degree of concordance among the two approaches. Value of particular heat ( $D_{qg}$ )

In nanomaterials, particular heat is described as the quantity of thermal energy needed to raise a unit

mass temperature by one degree Celsius. At the nanoscale, new behaviors develop a result of increased surface region, quantum phenomena, and confinement. The high surface area-to-volume ratio of nanomaterials, together with fundamental phenomena, can impact vibrational modes and hence change specific heat. In nanocomposites, confined mechanisms and interactions lead to more variations. The determined  $D_{qg}$  values for the Cu and Al film width are decreased and the metric always increases and numerical values for slimmer layers.

### 4.2 Values of Diffusivity ( $E_g$ )

The calculated heat diffusivity  $E_g$  values for the Cu and Al films in the 20–200 nm range are displayed in Fig. 3.

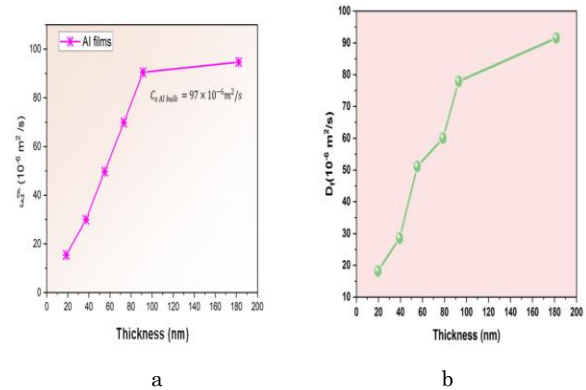


Fig. 3 – Thermal diffusivity: a) Al films and b) Cu films

Levels were found to be lower when the film width was possible and the produced oxide at room temperature prevented the Cu films from reaching their maximum diffusivity values throughout the experiments. Nonetheless, the films had a comparable propensity to get thicker.

### 4.3 Coefficients of Heat Conductivity ( $k_f$ )

The  $k_f$  measurements for Cu and Al films with thicknesses ranging at room temperature were calculated using Eq. (7). Comparable to  $E_g$ , growing tendency characteristic is seen as the depth grows. However, for Al films, the bulk thermal insulation while

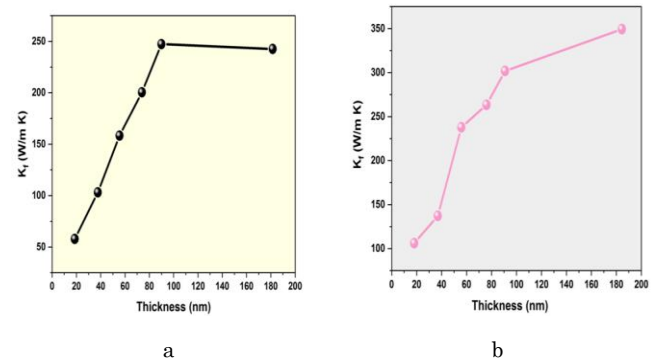


Fig. 4 – Thermal conductivity: a) Al films and b) Cu films

for Cu films, it achieves its optimum at 200 nm and the value is reached at 80 nm depth. Fig. 4 shows the heat conductivity between Al and Cu films. There is substantial concurrence when comparing published results for this metric obtained using different techniques. Nevertheless, data was discovered for the various physical characteristics for this thickness range.

## 5. CONCLUSION

In this study, the strong size-dependent behaviour is seen in the metallic thin films at tiny levels, involving the mechanical characteristics, micro structural stability, and the transition of deformation processes. Methods for determining different technological and conceptual

frameworks are proposed and discussed. For widths ranging from 20 to 200 nm, the Coefficients of heat conductivity ( $k_f$ ), particular heat ( $D_{gg}$ ), thermal diffusivity ( $E_g$ ), and temperature coefficient of resistance  $\alpha_r$  were reported for Al and Cu. We discuss the modulus of elasticity of AlCu alloys with nanometer-thickness. The material features are very different from the stated bulk principles, according to the findings of these determined attributes. As a result, to identify the various qualities at the nanoscale, new approaches and procedures must be proposed and developed. Determining the ranges of the physical attributes of components, including metallic materials, electronic components, and insulating materials, can be challenging in the field of material sciences.

## REFERENCES

1. Z. Zhang, Y. Ouyang, Y. Cheng, J. Chen, N. Li, G. Zhang, *Phys. Rep.* **860**, 1 (2020).
2. T.D. Frazer, J.L. Knobloch, K.M. Hoogeboom-Pot, D. Nardi, W. Chao, R.W. Falcone, M.M. Murnane, H.C. Kapteyn, J.N. Hernandez-Charpak, *Phys. Rev. Appl.* **11** No 2, 024042 (2019).
3. V. Syrovatko, Y. Syrovatko, *Mater. Proc.* **14** No 1, 35 (2023).
4. V. Dhyani, G. Ahmad, N. Kumar, S. Das, *IEEE Trans. Electron Dev.* **67** No 2, 558 (2020).
5. A. Ahmad, S. Mitra, S.K. Srivastava, A.K. Das, *J. Magn. Magn. Mater.* **15**, No 474, 599 (2019).
6. Y.G. Bi, Y.F. Liu, X.L. Zhang, D. Yin, W.Q. Wang, J. Feng, H.B. Sun, *Adv. Opt. Mater.* **7** No 6, 1800778 (2019).
7. M.A. Roudbari, T.D. Jorshari, C. Lü, R. Ansari, A.Z. Kouzani, M. Amabili, *Thin-Walled Structures* **170**, 108562 (2022).
8. T.D. Frazer, *Extreme Ultraviolet Measurements of Thermal and Elastic Dynamics In Nanostructured Media, Doctoral dissertation* (University of Colorado: 2019).
9. A.G. Mochugovskiy, A.V. Mikhaylovskaya, M.Y. Zadorognyy, I.S. Golovin, *J. Alloy. Compd.* **856**, 157455 (2021).
10. P. Shen, L. Lu, Y. He, F. Wang, S. Hu, *Cement Concrete Res.* **118**, 1 (2019).
11. S. Fan, X. Feng, Y. Han, Z. Fan, Y. Lu, *Nanoscale Horizons* **4** No 4, 781 (2019).
12. T. Zhao, C. Xu, W. Ma, Z. Liu, T. Zhou, Z. Liu, S. Feng, M. Zhu, N. Kang, D.M. Sun, H.M. Cheng, *Nat. Commun.* **24**, No 10, 4854 (2019).
13. X. Zhang, W. Li, H. Kou, J. Shao, Y. Deng, X. Zhang, J. Ma, Y. Li, X. Zhang, *J. Appl. Phys.* **125** No 18, 185105 (2019).

## Розмірно-залежні фізичні властивості металевих плівок: аналіз теплових і механічних характеристик у нанорозмірному режимі

S.R. Thorat<sup>1</sup>, V.M. Tidake<sup>2</sup>, P.M. Patore<sup>1</sup>, P.B. Khatkale<sup>3</sup>, A.A. Khatri<sup>4</sup>, P.M. Yawalkar<sup>5</sup>, S.S. Ingle<sup>1</sup>

<sup>1</sup> Department of Mechanical Engineering, Sanjivani College Engineering, Kopergaon, SPPU, Pune, India

<sup>2</sup> Department of MBA, Sanjivani College of Engineering, Kopergaon, SPPU, Pune, India

<sup>3</sup> Sanjivani University, Kopergaon, MH, India

<sup>4</sup> Department of Computer Engineering, Jaihind College of Engineering, Kuran, SPPU, Pune, MH, India

<sup>5</sup> Department of Computer Engineering, MET's Institute of Engineering, Nashi, India

Металеві плівки - тонкі шари металу, нанесені на поверхні, мають широкий спектр використання в багатьох секторах. Металеві плівки, як правило, виготовляються шляхом напилення або хімічного осадження з парової фази і відіграють важливу роль в електроніці, оптиці та покриттях. Їх фундаментальна провідність, відбивна здатність і здатність до адаптації є важливими для розробки інноваційних матеріалів і систем. Проведено дослідження жорсткості, оптичної відбивної здатності, температуропровідності та енергетичної рухливості металевих плівок. На вищевказані властивості впливає товщина шару, склад і процеси осадження. Розуміння складності цих фізичних особливостей має вирішальне значення для модифікації металевих плівок для конкретних застосувань, що стимулює технологічні та матеріалознавчі інновації. У цьому дослідженні були оцінені фізичні характеристики металевих плівок, товщина яких 20-200 нм. Запропоновано методи визначення температурно-залежних коефіцієнтів опору, теплопровідності, теплопровідності та теплопровідності плівок Cu, Al. Швидко нагрівання, яке спостерігається за короткий проміжок часу, дозволяє першочергово оцінити теплові характеристики металевого шару без впливу на підкладку.

**Ключові слова:** Металеві плівки, Термічні характеристики, Механічні характеристики, Нанорозмірні матеріали.